

A Contribution of X ray Diffraction Analysis in the Determination of Creep of Si_3N_4 Ceramics

Claudinei dos Santos^{a*}, Kurt Strecker^a, Francisco Piorino Neto^b,

Olivério Moreira Macedo Silva^b, Cosme Roberto Moreira da Silva^b

^aFaculdade de Engenharia Química de Lorena,

Departamento de Engenharia de Materiais, FAENQUIL-DEMAR,

Polo Urbo-Industrial, Gleba AI-6, s/n, C. P. 116, 12600-000 Lorena - SP, Brazil

^bCentro Técnico Aeroespacial, Divisão de Materiais, CTA-IAE/AMR,

Praça Marechal Eduardo Gomes, 50, 12228-904 São José dos Campos - SP, Brazil

Received: December 2, 2004; Revised: July 13, 2005

The understanding of the creep behavior of silicon nitride (Si_3N_4) is extremely complex because of a large number of parameters influencing simultaneously the creep deformation of the materials. In general, the main creep mechanisms acting in these materials are grain boundary sliding or materials transport by solution-precipitation process. In this work, the creep behavior has been monitored by X ray diffraction analysis, determining the peak intensity ratio of the (101) and (210) planes of $\beta\text{-Si}_3\text{N}_4$. This characterization technical, allied the microstructural analysis can contribute to determination of creep mechanisms acting in material. The $\beta\text{-Si}_3\text{N}_4$ grains are highly elongated with aspect ratios ranging between 3 and 11. Therefore, the intensity of the peaks related to the basal plane (101) tends to be higher when compared to the lateral planes (210). During creep deformation occurs alignment of the elongated $\beta\text{-Si}_3\text{N}_4$ grains in the plane parallel to the direction of the applied load, reflecting in the peak intensity ratio. Crept samples presented variations in the (101)/(210) peak intensity ratio of $\beta\text{-Si}_3\text{N}_4$ indicating that grain rotation can be contributing with creep deformation. In this way, the use of X ray diffractometry as a mean to characterize microstructural changes during creep has been shown successfully.

Keywords: X ray diffraction, creep mechanisms, Si_3N_4

1. Introduction

Si_3N_4 -based ceramics exhibit excellent high-temperature properties, such as high creep and oxidation resistance. These materials have been intensively investigated because of the possible substitution of steels, superalloys, etc. in high-temperature applications due to their higher corrosion, thermal shock and oxidation resistance¹⁻².

The study of the creep behavior of these materials is difficult, because different mechanisms can act, depending on the type of creep test (bending, tension or compressive tests), temperature and stress applied. Tensile creep generally occur by cavitation mechanism, while in the compressive tests, the major phenomena is grain boundary sliding. In the creep tests achieved around 1400 °C or in sintered Si_3N_4 ceramics with residual $\alpha\text{-Si}_3\text{N}_4$ content, the solution-precipitation mechanism can occur^{3,4}.

The specific phenomena occurring during creep deformation of hot-pressed $\beta\text{-Si}_3\text{N}_4$ ceramics in compressive tests, is the variation of anisotropy by preferential alignment of the elongated $\beta\text{-Si}_3\text{N}_4$ grains. This microstructural change by grain rotation during creep can be described quantitatively by X ray diffraction analysis, determining the relative peak intensity ratio between the planes (101) and (210) of $\beta\text{-Si}_3\text{N}_4$ ⁵.

In this work, the viability of this technique for the description of microstructural changes during compressive creep was analyzed. Four types of $\beta\text{-Si}_3\text{N}_4$ -based ceramics with distinct microstructural features were produced by hot-pressing and submitted to compressive creep testing. After testing, the anisotropy in the samples was determined by X ray diffraction, and correlated with microstructural aspects.

2. Experimental Procedure

2.1. Sample preparation

High purity Si_3N_4 (E10, UBE Industries-Japan, $\alpha\text{-Al}_2\text{O}_3$ (CR-6, BaikaloX-France), AlN (Grade Fine, H.C.Starck, Germany) and rare earth oxide solid solution (produced at FAENQUIL and with 50% Y_2O_3), designed RE₂O₃, were used as starting materials. Four types of ceramic materials were produced varying the additives and their respective relative amounts as presented in Table 1.

Powder batches were prepared by milling for 2 hours, using Al_2O_3 balls and ethanol media. The suspension were dried for 12 hours at 120 °C, and subsequently sieved through sieve 60 mesh for deagglomeration. The powder mixtures were compacted by uniaxial pressing under 50 MPa and subsequently by isostatic pressing under 300 MPa.

Hot-pressing was done at 1750 °C for 30 minutes under a pressure of 20 MPa with a heating rate of 15 °C/min in nitrogen atmosphere, obtaining sintered specimen of approximately 25 mm (diameter) x 7 mm (height). From these discs, samples of 6 x 3 x 3 mm³ were cut and used for creep testing.

The phase compositions of the sintered samples were determined by X ray diffraction of the polished surfaces. This analysis was conducted by a Phillips PW1380/80 diffractometer, using CuK_α radiation, at angles 2 θ ranging on 10 and 80°, step width of 0.02° and 5 seconds (exposure time per position).

*e-mail: claudinei@demar.fauenquil.br, clvr2@yahoo.com

2.2. Experimental apparatus used in creep tests

Compressive creep tests were carried in air using a dead-weight-creep-rupture machine. The compressive load was transmitted to the sample by high creep resistance SiC bars, and the length variation of the sample was measured using a linear variable differential transformer (LVDT) with a precision of 1 μm . The temperature was controlled to ± 2 $^{\circ}\text{C}$ using a Pt/Pt-10%Rh thermocouple.

Samples of $6 \times 3 \times 3 \text{ mm}^3$ were used in the creep tests. The compressive creep behavior of the samples has been investigated in the same axis as the hot-pressing direction. Due to the alignment of the elongated $\beta\text{-Si}_3\text{N}_4$ grains in planes perpendicular to the hot-pressing direction, an increasing creep resistance is expected for this orientation, when compared to specimen orientated perpendicular to the hot-pressing axis, because grain boundary sliding by viscous flow is more difficult. Figure 1 show the schematic apparatus used in the creep tests.

Compressive creep testing was done under air at different temperatures and stresses of 1300 $^{\circ}\text{C}$ - 300 MPa (SNCAL 5), 1275 $^{\circ}\text{C}$ - 200 MPa (SNCAL 20), 1340 $^{\circ}\text{C}$ - 200 MPa (SNCAN 5) and 1340 $^{\circ}\text{C}$ - 300 MPa, respectively.

2.3. X ray diffraction

X ray diffraction analysis has been used to verify a partial crystallization of the amorphous intergranular phase and possible variations of the α and $\beta\text{-Si}_3\text{N}_4$ amounts, due to the influence of creep. Furthermore, the degree of anisotropy has been determined by the (101) to (210) peak intensity ratio of $\beta\text{-Si}_3\text{N}_4$ in planes parallel and perpendicular to the hot-pressing axis, prior and after creep testing⁶⁻⁸. In this way differences in the alignment of the $\beta\text{-Si}_3\text{N}_4$ grains caused during creep can be verified and used for to contribute for the interpretation of the predominant creep mechanism.

2.4. SEM characterization

For microstructural analysis, the specimens were ground, polished and chemically etched by a 1:1 mixture of NaOH and KOH at 500 $^{\circ}\text{C}$ for 3 minutes. The grain size and the aspect ratio were determined by the statistical approximation proposed by Wötting et al.⁹ who considered that 10% of the grains are exactly parallel to the plane analyzed and, consequently, indicate the "real" aspect ratio of the grains. Approximately 1000 $\beta\text{-Si}_3\text{N}_4$ grains have been measured, choosing the 10% of the apparently largest grains for determination of the average width, length and aspect ratio of the grains. The orientation of the grains was evaluated by determining the angle θ between the c-axis of the $\beta\text{-Si}_3\text{N}_4$ grains and the x-axis of the planes normal and parallel to the hot-pressing direction⁶, see Figure 2.

3. Results and Discussion

3.1. Sample characterization

Table 2 presents the phase composition of the hot-pressed samples.

As can be seen, samples with Al_2O_3 as additive presented a complete transformation of α -into $\beta\text{-Si}_3\text{N}_4$, whereas AlN additions resulted in the formation of $\alpha\text{-SiAlON}$ (solid solutions of $\alpha\text{-Si}_3\text{N}_4$). Higher amounts of AlN lead to the formation of higher amounts of $\alpha\text{-SiAlON}$. These variations in the phase composition of the hot-pressed samples lead to specimen of different microstructures and also different creep behavior, as described in the following.

3.2. Characterization after creep tests

Steady state creep rate of the samples are summarized in Table 3.

Table 1. Composition of samples prepared.

Mixtures	Identification	Composition (in wt. (%))			
		Si_3N_4	Al_2O_3	AlN	RE_2O_3
$\text{Si}_3\text{N}_4 + 5 \text{ vol. \% } \text{RE}_2\text{O}_3 - \text{Al}_2\text{O}_3$	SNCAL 5	92.00	2.85	-	5.15
$\text{Si}_3\text{N}_4 + 20 \text{ vol. \% } \text{RE}_2\text{O}_3 - \text{Al}_2\text{O}_3$	SNCAL 20	70.76	10.44	-	18.80
$\text{Si}_3\text{N}_4 + 5 \text{ vol. \% } \text{RE}_2\text{O}_3 - \text{AlN}$	SNCAN 5	93.54	-	3.54	2.92
$\text{Si}_3\text{N}_4 + 20 \text{ vol. \% } \text{RE}_2\text{O}_3 - \text{AlN}$	SNCAN 20	75.30	-	13.52	11.18

Table 2. Characteristic of the hot-pressed samples.

Composition	Crystalline phases	α' : β phase relationship
SNCAL 5	$\beta\text{-Si}_3\text{N}_4$	00:100
SNCAL 20	$\beta\text{-Si}_3\text{N}_4$	00:100
SNCAN 5	$\beta\text{-Si}_3\text{N}_4$; $\alpha\text{-SiAlON}$	90:10
SNCAN 20	$\alpha\text{-SiAlON}$	100:00

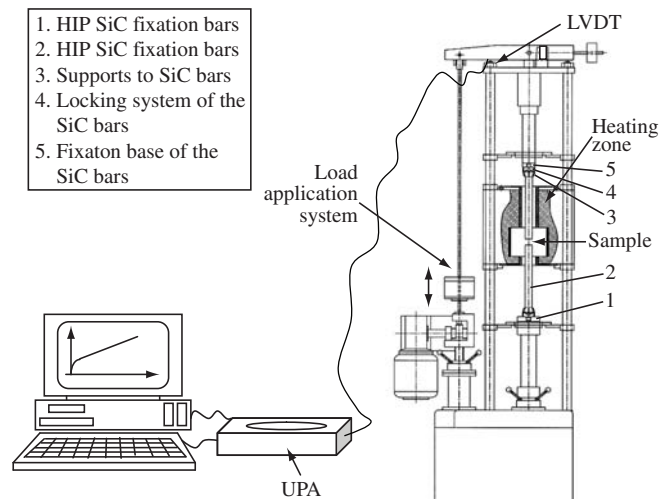


Figure 1. Schematic compressive creep tests apparatus.

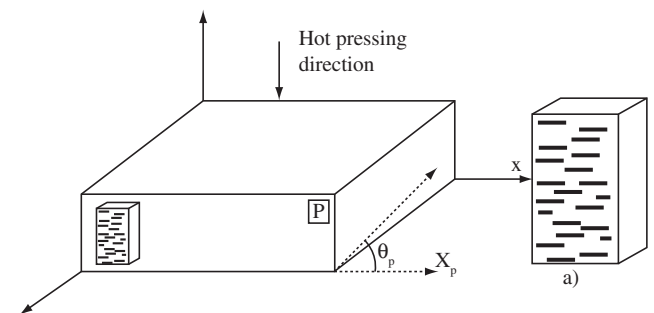


Figure 2. Schematic figure of a hot-pressed sample with preferential grain orientation in the plane parallel to the hot pressing direction (P). θ_p represents the angle of grain orientation in the P plane.

Table 3. Creep results of the hot pressed samples.

Composition	Tests conditions		Steady state creep rate ($\dot{\epsilon}_{ss}$) - h^{-1}
	Temperature ($^{\circ}\text{C}$)	Stress (MPa)	
SNCAL 5	1300	300	1.2×10^{-3}
SNCAL 20	1275	200	1.3×10^{-3}
SNCAN 5	1340	200	9.0×10^{-4}
SNCAN 20	1340	300	2.5×10^{-4}

It is important to recall that samples with Al_2O_3 as additive, SNCAL 5 and SNCAL 20, exhibited only $\beta\text{-Si}_3\text{N}_4$ as crystalline phase, see Table 2. Therefore, solution-precipitation phenomena during creep deformation of these samples can be excluded. On the other hand, $\alpha\text{-SiAlONs}$ are subject to solution-precipitation at relatively low temperatures when submitted to compressive stresses¹⁰. In this case grains regions subjected to intensive compressive stresses are dissolved and precipitate in regions of tensile stress, thus promoting reorientation of these grains and considerable morphological changes.

Crept samples were grinded and polished, and analyzed by X ray diffractometry. As preferential grain alignment takes place in the plane parallel to the hot pressing direction, phases analysis was conducted exclusively in this plane. In general, samples of identical composition crept under different conditions did not presented significant changes. Figure 3 presents X ray diffraction patterns for each composition studied.

As can be seen, only sample SNCAL 20 showed partial crystallization of the intergranular phase after creep testing. Sample SNCAL 5 and, specially, samples containing AlN as additives, denominated SNCAN, did not show crystalline intergranular phases. Furthermore, the amount of $\alpha\text{-SiAlON}$ formed in samples SNCAN did not change during creep, indicating that under the creep conditions applied (temperatures at 1340°C) no significant reconstructive phase transformation of α' -into β' -did occur.

Another important parameter that can be obtained by X ray diffraction analysis is the alignment of grains in planes parallel to the hot-pressing direction, calculating the relative peak intensity of the (101) and (210) planes of $\beta\text{-Si}_3\text{N}_4$ ($I_{(101)/(210)}$). These results are discussed considering previously published results in order to establish the acting creep mechanism.

3.3. Creep mechanism

According to Lange et al.³, Si_3N_4 based ceramics with small quantities of intergranular glassy phase exhibit a stress exponent n of about unity, corresponding to diffusional creep. Also, other works relate the creep of Si_3N_4 ceramics to diffusional process^{3,4,11-15}. In the presence of a residual glassy phase, grain sliding can be accommodated by diffusion of viscous flow or solution-precipitation of grains. Grain sliding by viscous flow is probably the principal mechanism in the samples investigated in this study, under compressive creep conditions. As mentioned before, determination of the anisotropy in planes parallel to the hot-pressing direction is based on X ray diffraction analysis of the peak intensity ratio of the planes (101) and (210) of $\beta\text{-Si}_3\text{N}_4$. The texturization observed in hot-pressed Si_3N_4 ceramics is due to two basic mechanisms: grain rotation and preferential grain growth because of the stress gradient. Due to the preferential alignment of grains already during hot-pressing, different peak intensity ratios of the (101) and (210) planes of $\beta\text{-Si}_3\text{N}_4$ are observed in the samples prior to the creep testing, depending on their composition.

For example, in Figure 4, the changes in the peak intensity ratio $I_{(101)/(210)}$ prior and after creep testing are shown for both planes, paral-

lel, P, and perpendicular, N, to the hot-pressing direction direction of samples SNCAL 5. As can be seen from the X ray diffraction patterns plane P presents a high variation in the peak intensity ratio when compared to plane N, prior to creep testing. The ratio is 1.39 for plane P and 0.40 for plane N. These ratios indicate preferential grain alignment in Plane N, because of the uniaxial hot-pressing process applied for densification of these materials.

After creep testing at 1300°C under a stress of 300 MPa it can be noted that the peak intensity ratio of plane P increased to 1.71, indicating that further alignment of the grains by rotation occurred during creep. On the other hand, the peak intensity ratio of plane N remained almost unaltered. For samples SNCAL 20, submitted to creep at 1275°C under 250 MPa the peak intensity ratio for plane P increased from 1.1 to 1.75, also indicating that further alignment of grains by rotation occurred.

As the quantity of intergranular phase in these samples (SNCAL 20) is much higher as in samples SNCAL 5, it is reasonable to assume that the process of grains sliding and grain rotation are easier to occur. Further considering that a considerable amount of this intergranular phase is susceptible to oxidation, and previously reported¹⁶, it can be inferred that by migration of part of this intergranular phase to the sample surface cavitations are generated inside, resulting in increased creep rates. Observing the external aspects of the specimens SNCAL 20¹⁶, it can be noted that they suffered oxidation at a much larger scale than specimen SNCAL 5.

The technique to describe the texture by the peak intensity ratio of $\beta\text{-Si}_3\text{N}_4$, permits only to evaluate microstructural features of $\beta\text{-Si}_3\text{N}_4$. Previous works¹⁷ showed that this method is not efficient for $\alpha\text{-SiAlON}$ ceramics, which also exhibit the most intensive peaks for the planes (101) and (210).

Some creep experiments of specimen SNCAL 5, SNCAL 20 and SNCAN 5 were interrupted at different times, in order to describe the alignment of grains in relation to the time of the creep experiments. The results are presented in Figure 5.

Yoon et al.⁸ reported that the maximum peak intensity ratio $I_{\beta\text{-Si}_3\text{N}_4}$ in anisotropic $\beta\text{-Si}_3\text{N}_4$ ceramics equal 1.76 in the plane parallel to the hot-pressing axis. The results shown in Figure 5 indicate that during creep occurs a continuous alignment of grains due to the applied compressive stress promoting rotation of grains and coursing creep deformation. The Figure 6 indicates this behavior.

The increasing values of $I_{(101)/(210)}$ with increasing time indicate that the reorientation of grains is a continuous process until its maximum is reached. Probably, from this moment, the ceramic bodies are subjected to increasing cavitation, further increasing creep deformation.

Table 4 presents the most important crystallographic characteristics and microstructural features of the crept materials.

Regarding the previously exposed results, it can be suggested that the main creep mechanism acting in the specimen investigated in this work are:

Sample sintered with $\text{Al}_2\text{O}_3/\text{RE}_2\text{O}_3$ as additives presented distinct microstructural characteristics, depending on the quantity of additives used. Increased average grain sizes with higher aspect ratios were observed in these materials. On the other hand, the hot-pressing process produced a microstructure less anisotropic for samples of composition SNCAL 20. Compressive creep of these specimen with larger grain sizes, smaller anisotropy and high amounts (20%) of amorphous intergranular phase, caused higher deformation and also severe oxidation, when compared to samples SNCAL 5. The differences observed in the stress exponent between samples SNCAL 20 and SNCAL 5, ranging between 1.7 and 2.5 or between 0.7 and 1.0, respectively, can be related to the different composition of the intergranular phase, resulting in different oxidation resistance.

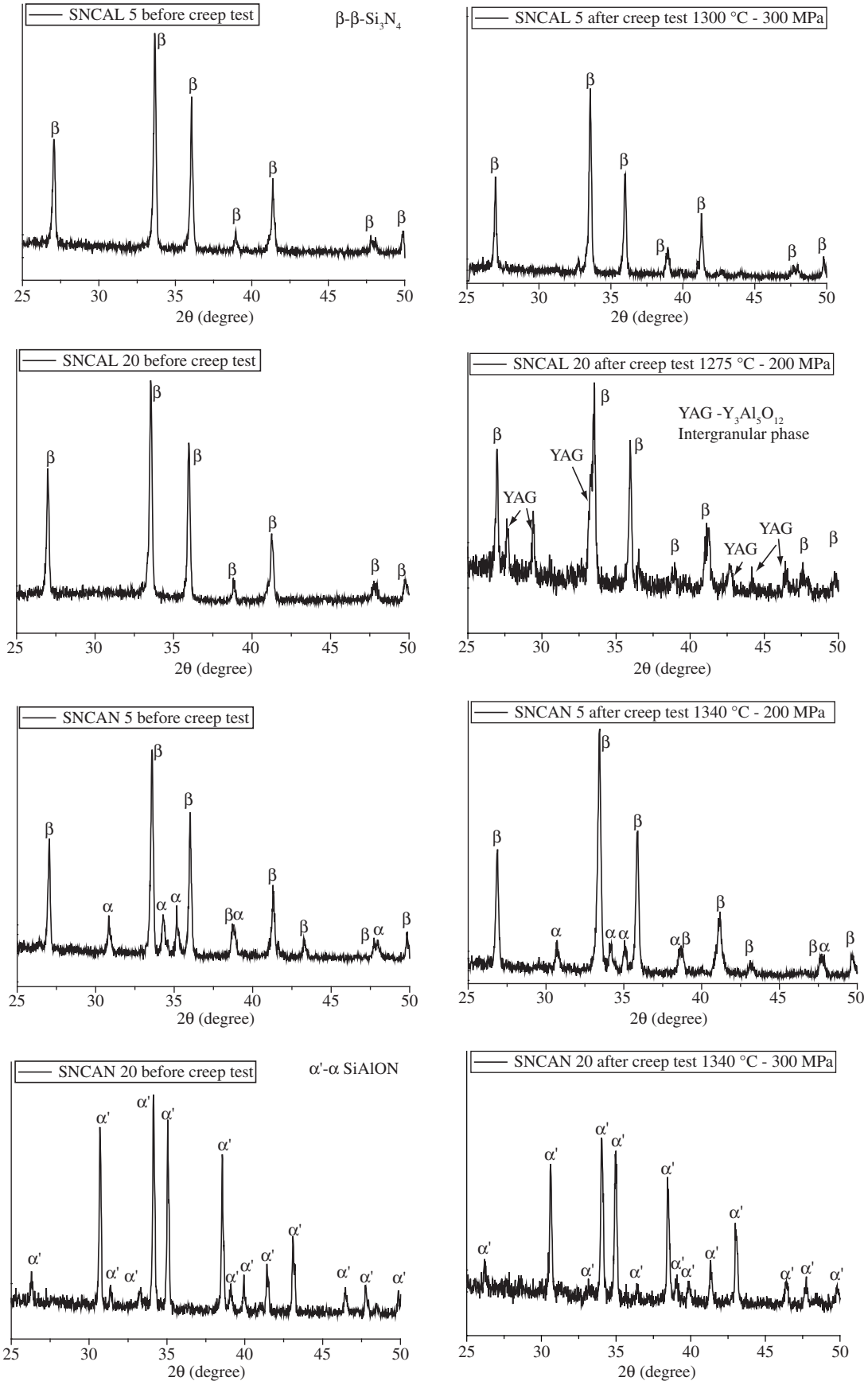


Figure 3. X ray diffraction patterns of the composition studied.

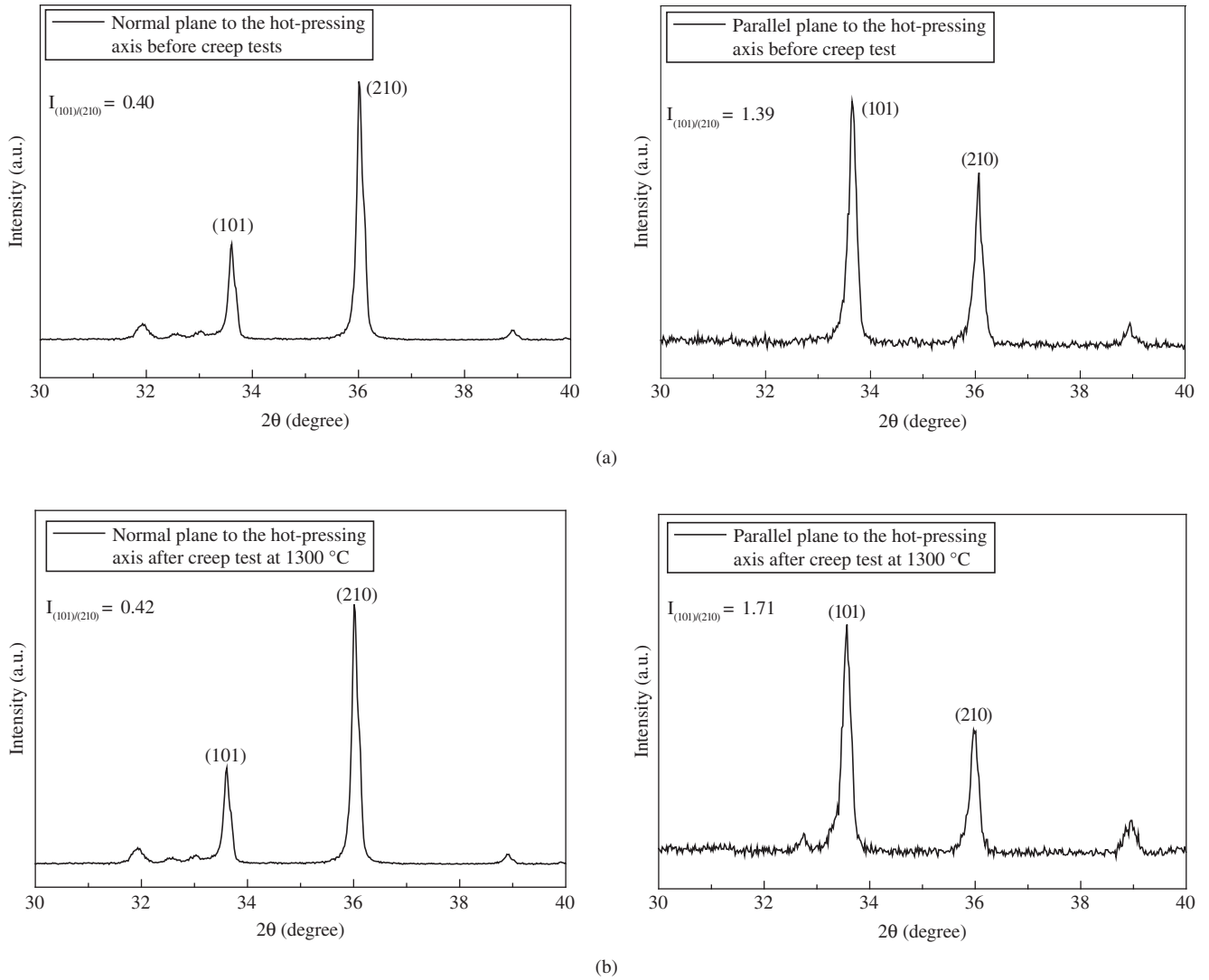


Figure 4. X ray diffraction patterns of the specimens: a) before he creep tests, in perpendicular and parallel planes to the hot pressing axis; and b) after creep tests at 1300 °C and 300 MPa, in planes (N) and (P).

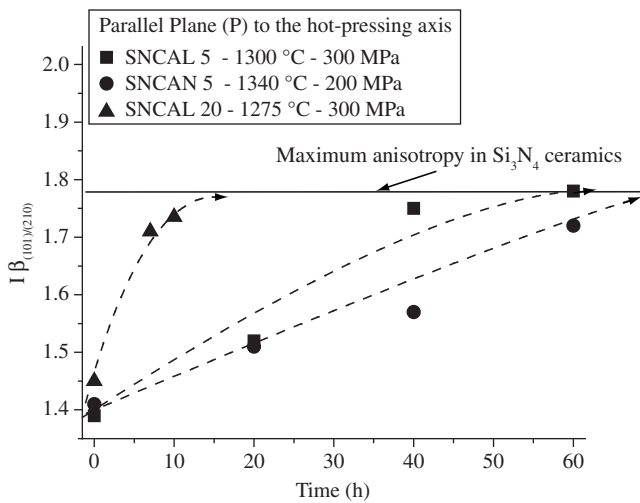


Figure 5. Reorientation of the $\beta\text{-Si}_3\text{N}_4$ grains of the compositions SNCAL 5, SNCAL 20 and SNCAN 5 as a function of the exposure time to the creep deformation.

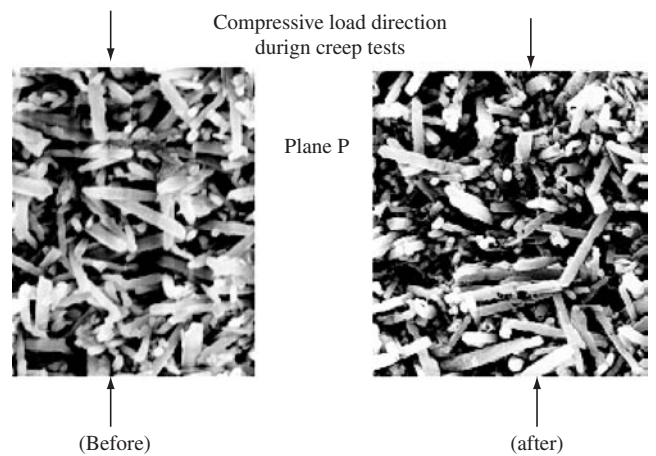


Figure 6. SEM micrographs of the sample SNCAL 20 in the P and N planes, before and after the creep test.

Table 4. Typical characteristics of the intergranular phases, microstructures and crystalline phases of the crept samples.

Composition	Intergranular Phases			θ_p (°)		Microstructural Aspects			
	% in volume	Chemical composition of the intergranular phase (in wt. (%))	Possibles crystalline intergranular phases	Before	After	Before		After	
				Grain size Average (μm)	Aspect Ratio	Grain Size Average (μm)	Aspect Ratio		
SNCAL 5	5%	27.4 (Al_2O_3); 49.4 (Y_2O_3); 23.2 (SiO_2)	$\text{Y}_3\text{Al}_5\text{O}_{12}$, $\text{Y}_2\text{Si}_3\text{N}_4\text{O}_3$, YSiO_2N	12.9 ± 14.0	11.4 ± 13.0	2.5	6.5	2.6	6.4
SNCAL 20	20%	33.6 (Al_2O_3); 60.4 (Y_2O_3); 6.0 (SiO_2)	$\text{Y}_3\text{Al}_5\text{O}_{12}$, $\text{Y}_2\text{Si}_3\text{N}_4\text{O}_3$, YSiO_2N	35.1 ± 23.5	16.5 ± 15.0	4.1	11.2	3.9	11.0
SNCAN 5	< 5%	-	Y_2O_3 , $\text{Y}_3\text{Al}_5\text{O}_{12}$ residual	16.8 ± 15.0	10.6 ± 12.7	-	6.2	-	5.9
SNCAN 20	<<< 20%	-	$\text{Y}_3\text{Al}_5\text{O}_{12}$	N.A.	N.A.	2.9	3.8	2.5	3.3

Despite this, the mechanism of creep deformation of these materials are associated to diffusional process. The X ray diffraction patterns indicate an alignment of the grains in the axis parallel to the hot-pressing direction, demonstrating that grain boundary sliding occurred. The absence of α - Si_3N_4 and the microstructural aspects listed in Table 4, showing that no significant modifications in the morphology of the Si_3N_4 grains occurred during creep, presumably reduces the importance of solution-precipitation process for the creep behavior of these ceramic materials. Therefore, it can be assumed that grain sliding by viscous flow is the predominant creep mechanism under the stress and temperatures applied in this work.

Samples of composition SNCAN 5, presenting a high amount of β - Si_3N_4 and a considerable amount of residual intergranular phase are also subjected to creep deformation by grain sliding. Variations of the stress exponent and activation energy are expected because of the microstructural and crystallographic differences and because of the different amorphous intergranular phases. It is assumed by the results of characterization that the preferential acting creep mechanism is probably grain sliding, because the microstructures indicate an effective alignment of grains in the plane parallel to the hot-pressing direction. This observation is supported by the variations measured in the peak intensity ratios of the (101) and (210) planes of β - Si_3N_4 .

The microstructural aspects (see Table 4) demonstrate that in samples of composition SNCAN 20 considerable microstructural changes occurred, supposedly by solution-precipitation process being the predominant mechanism of creep deformation for these specimens, resulting in a lower grain boundary density per area. These samples of diminished grain boundaries and smaller amount of intergranular phase are less susceptible to oxidation, in accordance to the lower creep rates of these samples when compared to the others.

Considering the results of stress exponent, activation energy and microstructure it is assumed that the predominant mechanism for creep deformation of this material is by the solution-precipitation process of these Si_3N_4 phase, which is dissolved at the interfaces under pressure in the viscous, vitreous phase, transported to regions of induced tensile stress where it precipitates, generating irregular surfaces as observed in the microstructures. Besides this mechanism the rotation of certain grains by grain boundary sliding should be considered.

4. Conclusions

In this work, X ray diffraction analysis has been used to contribute for the characterization of the creep behavior in compression of Si_3N_4 based ceramics. The alignment of grains during compressive

creep deformation has been determined by the variation in the peak intensity ratio of the (101) and (210) planes of β - Si_3N_4 . It was possible to observe that changes in the relative peak intensity ratio, which were caused by the reorientation of the grains in the plane parallel to the hot-pressing axis during compressive creep, indicating that grain boundary sliding occurred. It has been demonstrated that X ray diffraction analysis is an efficient method to characterize this phenomena. Furthermore it was possible by comparison of the X ray diffraction patterns of samples prior and after creep testing that the solution-precipitation mechanism was not of great importance for the compressive creep behavior of these materials, under the conditions applied in this work.

Acknowledgments

The authors thank FAPESP for financial support, granted under process n° 01/08682-6.

References

1. Bellosi A. Design and Process of non-oxide ceramics – case study: factor affecting microstructure and properties of silicon nitride. In: Gogotsi YG, Andrieuski RA, editors. *Materials Science of carbides, nitrides and borides*. Netherlands: Kluwer Academic Publishers; 1999. p. 285-304.
2. Riley FL. Silicon nitride and related materials. *Journal of the American Ceramic Society*. 2000; 83(2):245-265.
3. Lange FF, Davis BI, Clarke DR. Compression Creep of Si_3N_4 -MgO Alloys. *Journal of Material Science*. 1980; 15(3):601-610.
4. Wiederhorn SM, Hockley BJ, French JD. Mechanisms of deformation of silicon nitride and silicon carbide at high temperatures. *Journal of the European Ceramic Society*. 1999; 19(13-14):2273-2284.
5. Lee F, Bowman KJ. Texture and Anisotropy in Silicon Nitride. *Journal of the American Ceramic Society*. 1992; 75(7):1748-1755.
6. Santos C, Strecker K, Baldacim SA, Silva OMM, Silva CRM. Influence of additive content on the anisotropy in hot-pressed Si_3N_4 ceramics using grain orientation measurements. *Ceramics International*. 2004; 30(5):653-659.
7. Santos C. *Prensagem à quente de cerâmicas de Si_3N_4 com misturas de $\text{CTR}_2\text{O}_3/\text{AlN}$ e $\text{CTR}_2\text{O}_3/\text{Al}_2\text{O}_3$ como aditivos: caracterização microestrutural, comportamento mecânico e resistência à fluência*. [Doctoral thesis]. Lorena: Faculdade de Engenharia Química de Lorena; 2004.
8. Yoon SY, Akatsu T, Yasuda E. Anisotropy of creep deformation rate in hot-pressed Si_3N_4 with preferred orientation of the elongated grains. *Journal of Materials Science*. 1997; 32(14):3813-3819.
9. Wötting G, Kanka B, Ziegler G. In: Hampshire S, editor. *Non-Oxide Technical and Engineering Ceramics*. London: Elsevier; 1986. p. 83-96.

10. Rosenflanz A. Glass-reduced SiAlONs with improved creep and oxidation resistance. *Journal of the American Ceramic Society*. 2002; 85(9):2379-2381.
11. Silva CRM. *Compressive Creep of Silicon Nitride*. [Doctoral thesis]. Manchester: University of Manchester; 1989.
12. Evans RW, Wilshire B. *Introduction to Creep*. London: The Institute of Materials; 1993.
13. Crampon J, Duclos R. Compressive creep and creep failure of $8\text{Y}_2\text{O}_3/3\text{Al}_2\text{O}_3$ -doped hot-pressed silicon nitride. *Journal of the American Ceramic Society*. 1997; 80(1):85-91.
14. Yoon SY-, Akatsu T, Yasuda E. The microstructure and creep deformation of hot-pressed Si_3N_4 with different amounts of sintering additives. *Journal of the Materials Research*. 1996; 11(1):120-126.
15. Arellano-López AR, Varela-Feria FM, Martínez-Fernández J, Singh M. Compressive creep of silicon nitride with different secondary phase compositions. *Materials Science and Engineering A*. 2002; 332(1-2):295-300.
16. Santos C, Strecker K, Piorino Neto F, Lanna MA, Silva OMM, Silva CRM. Oxidation behavior of hot-pressed Si_3N_4 ceramics using Cr_2O_3 -AlN and Cr_2O_3 - Al_2O_3 as sintering additives. *Materials Science Forum*. 2005; 499:569-574.
17. Shin IH, Kim DJ. Growth of elongated grains in α -SiAlON ceramics. *Materials Letters*. 2001; 47(1):329-333.